Published online: June 6, 2018

Scientific Report

SOURCE DATA | TRANSPARENT PROCESS

EMBO reports

YAP and TAZ are essential for basal and squamous cell carcinoma initiation

Maud Debaugnies[1,†], Adriana Sánchez-Danés[1,†], Sandrine Rorive[2], Maylis Raphaël[1], Mélanie Liagre[1], Marie-Astrid Parent[1], Audrey Brisebarre[1], Isabelle Salmon[2] & Cédric Blanpain[1,3,*]

Abstract

YAP and TAZ are key downstream regulators of the Hippo pathway, regulating cell proliferation and differentiation. YAP and TAZ activation has been reported in different cancer types. However, it remains unclear whether they are required for the initiation of major skin malignancies like basal cell carcinoma (BCC) and squamous cell carcinoma (SCC). Here, we analyze the expression of YAP and TAZ in these skin cancers and evaluate cancer initiation in knockout mouse models. We show that YAP and TAZ are nuclear and highly expressed in different BCC types in both human and mice. Further, we find that cells with nuclear YAP and TAZ localize to the invasive front in well-differentiated SCC, whereas nuclear YAP is homogeneously expressed in spindle cell carcinoma undergoing EMT. We also show that mouse BCC and SCC are enriched for YAP gene signatures. Finally, we find that the conditional deletion of *YAP* and *TAZ* in mouse models of BCC and SCC prevents tumor formation. Thus, YAP and TAZ are key determinants of skin cancer initiation, suggesting that targeting the YAP and TAZ signaling pathway might be beneficial for the treatment of skin cancers.

Keywords basal cell carcinoma; cancer; squamous cell carcinoma; YAP; TAZ
Subject Categories Cancer; Signal Transduction
DOI 10.15252/embr.201845809 | Received 16 January 2018 | Revised 4 May 2018 | Accepted 14 May 2018 | Published online 6 June 2018
EMBO Reports (2018) 19: e45809

Introduction

Non-melanoma skin cancers, including basal cell carcinoma (BCC) and squamous cell carcinoma (SCC), are the most frequently diagnosed human cancers [1,2]. Basal cell carcinoma and squamous cell carcinoma represent a major health concern due to their high incidence, which is estimated to increment in the future due to increased sun exposure in Western countries. Therefore, there is an urgent need to identify the genes and signaling pathways controlling BCC and SCC initiation and progression.

YAP and TAZ are the major effectors of the Hippo signaling pathway, which regulates organ size, tissue homeostasis, regeneration, and tumorigenesis [3–5]. YAP and TAZ are two transcriptional co-activators that shuttle between the nucleus and the cytoplasm [6]. In the nucleus, YAP and TAZ interact with transcriptional factors of the TEA domain family members (TEAD) and induce the expression of proliferative and anti-apoptotic genes. The translocation of YAP and TAZ in the nucleus is determined by their phosphorylation state. YAP and TAZ translocate to the nucleus, where they activate their target genes, when they are hypophosphorylated; and remain in the cytoplasm when they are phosphorylated by LATS1 and LATS2. YAP and TAZ act as mechanosensors and can be activated by mechanical and physical cues originated by the microenvironment irrespective of Hippo pathway activation [7].

YAP and TAZ activation has been described in several solid tumors. It has been proposed that YAP and TAZ act as oncogenes through activation of target genes that promote acquisition of cancer stem cell properties, proliferation, chemoresistance, epithelial-to-mesenchymal transition (EMT), and metastasis [3–5,8]. Recent studies in the intestine have suggested that YAP and TAZ may function as tumor suppressor or oncogene depending on their cellular localization. Nuclear YAP and TAZ may be involved in WNT-associated intestinal transformation acting as an oncogene [9], whereas cytoplasmic YAP and TAZ may function as tumor suppressors by inhibiting the WNT/β-catenin signaling pathway, through the recruitment of BTRCP to the destruction complex leading to β-catenin degradation [10]. In hematological malignancies, including multiple myeloma, lymphoma, and leukemia, it has been proposed that YAP may function as tumor suppressor gene by activating pro-apoptotic genes [11].

During skin epidermis development, YAP is expressed and nuclear in epidermal progenitors, whereas it is localized in the cytoplasm in differentiated suprabasal cells [8,12]. Deletion of *YAP* in the basal epidermal cells during development results in neonatal lethality due to skin barrier defect, caused by a defect in proliferation of basal cell progenitors leading to thin/hypoplastic epidermis [8]. In contrast, overexpression of the nuclear form of YAP in adult basal epidermal cells leads to thickening of the skin, which is caused by expansion of basal epidermal compartment and abrogation of epidermal differentiation marker expression [8].

1 Laboratory of Stem Cells and Cancer, Université Libre de Bruxelles, Brussels, Belgium
2 Department of Pathology, Erasme University Hospital, University Libre de Bruxelles, Brussels, Belgium
3 WELBIO, Université Libre de Bruxelles, Brussels, Belgium
*Corresponding author. Tel: +32 2555 4175; E-mail: cedric.blanpain@ulb.ac.be
†These authors contributed equally to this work

YAP and *TAZ* deletion in adult skin epidermis leads to defect of hair follicle regeneration and wound healing [13]. These studies indicate that nuclear YAP enhances proliferation of epidermal stem and progenitor cells.

YAP and TAZ activation has been associated with skin tumorigenesis [14]. Nuclear YAP was reported in human BCC [15,16]. However, the functional role of YAP and TAZ during BCC initiation has not been reported yet. Nuclear YAP expression has been reported in different types of SCCs, including cutaneous, cervix, esophagus, and head and neck SCCs [8,17–25]. α-Catenin deletion in bulge stem/progenitor cells leads to cutaneous SCC formation and nuclear localization of YAP [18]. Overexpression of the nuclear form of YAP during embryonic development in epidermal cells followed by skin grafting leads to squamous skin tumor formation [8]. Deletion of YAP and TAZ in basal epidermal cells in a chemical-induced model of skin tumors leads to almost complete abrogation of papilloma formation, indicating that YAP and TAZ are required for the formation of benign skin tumors [24]. YAP depletion in a mouse xenograft model of cutaneous SCC inhibits tumor growth, suggesting that YAP could be important for SCC maintenance [25]. However, it remains unclear whether YAP and TAZ are required and necessary for the initiation of malignant SCCs.

Here, we assessed the role of YAP and TAZ in BCC and SCC initiation. We found that YAP and TAZ are expressed in the nucleus of different histological subtypes of BCCs and SCCs in both human and mice. BCC and SCC also expressed high level of YAP gene signatures, consistent with the activation of this pathway in these skin cancers. Deletion of YAP and TAZ in oncogene-targeted cells prevents BCC and SCC initiation. This study demonstrates that YAP and TAZ are key determinants of skin cancer initiation.

Results and Discussion

Nuclear YAP and TAZ expression in mouse and human BCC

To assess the role of YAP and TAZ signaling in skin tumors, we first assessed the expression and cellular localization of YAP and TAZ in two genetic BCC mouse models. Deletion of the *Patched1 (Ptch1)* gene in the basal epidermal cells leads to BCC arising mainly from the infundibulum and to a lower extent from the hair follicle and interfollicular epidermis [26–29], whereas activation of a constitutive form of the *Smoothened* (*SmoM2*) receptor using the *K14CREER* leads to BCC arising from the interfollicular epidermis (IFE) and infundibulum [30,31] . YAP and TAZ immunostaining in BCC arising following *Ptch1* deletion or *SmoM2* expression showed nuclear expression of YAP and TAZ in BCC from both mouse models (Fig 1A and B), suggesting that YAP signaling and TAZ signaling are active in mouse BCCs.

To determine the human relevance of our findings, we performed YAP and TAZ immunohistochemistry in different types of human BCCs. We found nuclear YAP expression in the majority of superficial, nodular, and infiltrative BCCs (Fig 1D). In contrast, only few epidermal basal cells stained positive for nuclear YAP in the epidermis from control individuals (Fig 1C). TAZ was expressed in some parts of superficial and nodular BCC and in the majority of infiltrative BCCs (Fig 1F). Altogether, these results reveal that nuclear expression of YAP and TAZ is a common feature of mouse and human BCCs, irrespective of the oncogene or tumor suppressor gene mediating BCCs initiation or the histological subtype of BCC. Somatic mutations that lead to YAP activation have been described in human BCCs [32]. These mutations occur in genes regulating YAP and TAZ phosphorylation (*LATS1* and *LATS2*) (28%) and their translocation from the nucleus to the cytoplasm (*PTN14*) (23%) [32]. However, the absence of these mutations in 50% of BCC contrasts with the presence of nuclear YAP in all BCCs, suggesting that other non-genetic mechanisms may lead to YAP activation in BCC.

Nuclear YAP and TAZ expression in mouse and human SCC

To define the role of YAP and TAZ signaling in skin SCCs, we analyzed the expression of YAP and TAZ in a mouse model of SCC that leads to the generation of SCCs with different degree of squamous differentiation and EMT [33–35]. Activation of oncogenic $Kras^{G12D}$ in combination with *Tp53* deletion in hair follicle lineage (using *Lgr5CREER/*$Kras^{G12D}$*/Tp53KO* mice) results in the generation of a wide spectrum of SCC, ranging from well-differentiated SCCs that present squamous differentiation to tumors that underwent EMT forming mesenchymal-like SCC resembling spindle cell carcinoma [33–36]. We observed nuclear YAP and TAZ expression at the leading edge of the invasive front of well-differentiated SCC. In contrast, mesenchymal-like SCC presented homogeneous nuclear YAP and TAZ staining (Fig 1G). These data indicate that YAP is expressed at the leading edge of well-differentiated SCCs and is even more strongly expressed in SCC presenting EMT, consistent with the notion that YAP promotes EMT [33,37,38]. The exact mechanisms by which YAP and TAZ are activated during cutaneous SCC formation are not well understood. Deletion of α-catenin, an adherens junction protein leads to cutaneous SCC formation in mice [18]. In this mouse model, Yap1 is found in the nucleus [8,18], and coimmunoprecipitation experiments showed that Yap1 interacts with α−catenin [8], suggesting that α-catenin may regulate the nuclear localization of Yap1. Further studies will be required to elucidate the additional mechanisms triggering YAP and TAZ activation during SCC initiation.

To investigate the relevance of these findings to human SCC, we assessed the expression and localization of YAP and TAZ in different SCCs from different anatomical sites. Actinic keratosis, which represents a pre-neoplastic lesion of human cutaneous SCC, showed a weak nuclear YAP staining (Fig 1E). In contrast, well-differentiated human SCC presented nuclear YAP expression at the invasive front and poorly differentiated SCCs with mesenchymal features showed a homogeneous stronger nuclear staining (Fig 1H). TAZ is found to be expressed mainly in the cytoplasm of a subset of well-differentiated and poorly differentiated SCC. Few cells stained positive for nuclear TAZ (Fig 1H). Those observations are consistent with the observations made in mouse SCC that YAP and TAZ are expressed in the nucleus of human SCCs and that stronger nuclear YAP staining is associated with more invasive tumor phenotype. To determine whether YAP and TAZ activation was a common feature of SCCs arising from different body locations independently of their tissue of origin, we performed IHC for YAP and TAZ in SCC from esophagus, head and neck, lung, and cervix. We observed nuclear YAP and TAZ staining in the different SCC types (Fig 1I). Altogether, these findings indicate that YAP signaling and

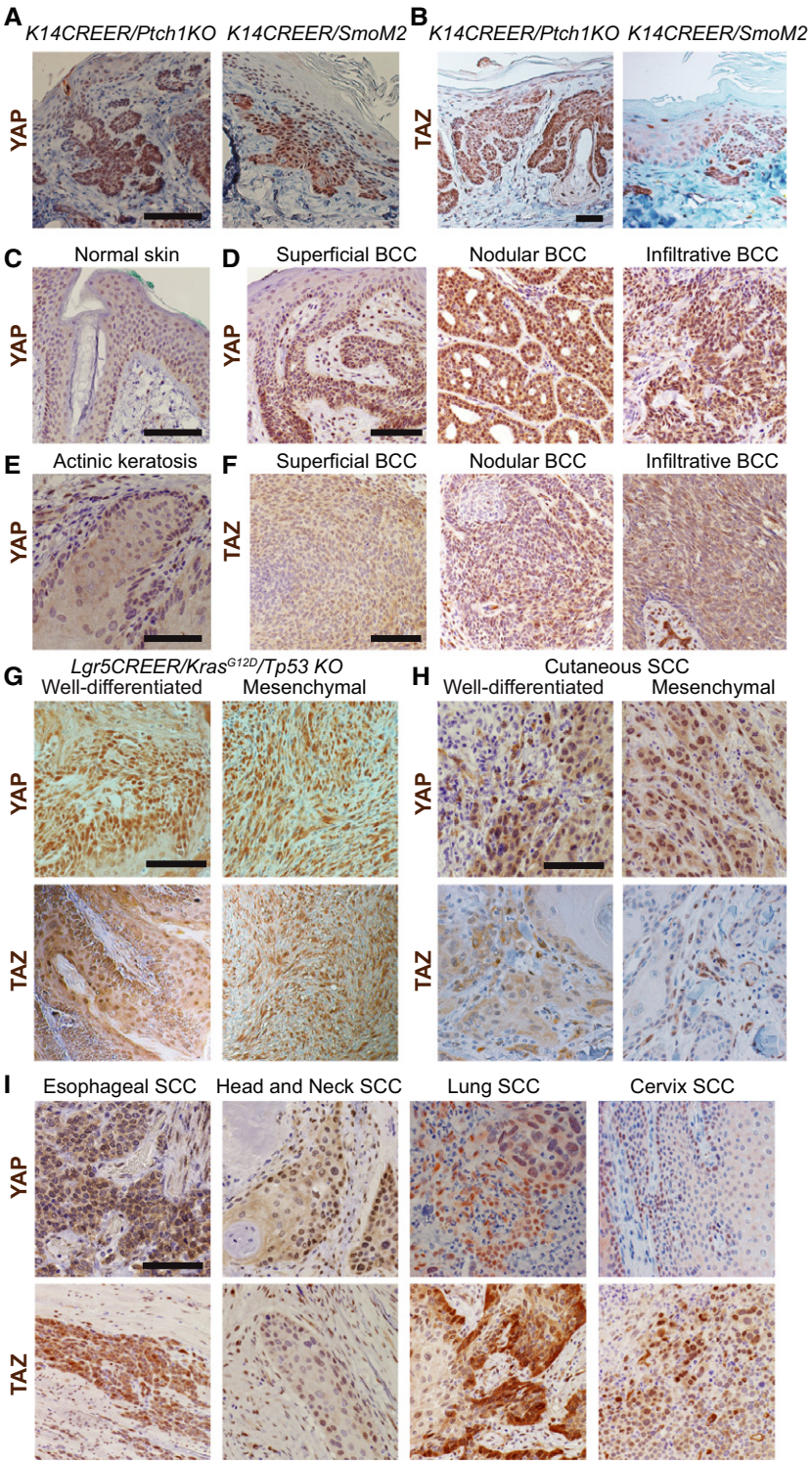

Figure 1. Nuclear expression of YAP and TAZ in mouse and human BCC and SCC.

A, B Immunohistochemistry for YAP (A) and TAZ (B) in mouse BCC from *Ptch1KO* and *SmoM2* models.

C, D Immunohistochemistry for YAP in human normal skin (C) and in human superficial, nodular, and infiltrative BCCs (D).

E Immunohistochemistry for YAP in human actinic keratosis.

F Immunohistochemistry for TAZ in human superficial, nodular, and infiltrative BCCs.

G Immunohistochemistry for YAP and TAZ in well-differentiated and mesenchymal SCC from *Lgr5CREER/Kras^{G12D}/Tp53 KO* mouse model.

H, I Immunohistochemistry for YAP and TAZ in human cutaneous SCC (H) and in human esophageal, head and neck, lung and cervix SCC (I).

Data information: Scale bars: 100 μm.

TAZ signaling are active in human SCCs, although more strongly in more invasive SCCs.

BCC and SCC express YAP gene signatures

To assess the transcriptional impact of the active YAP signaling in BCC and SCC, we performed GSEA of the genes upregulated in BCCs and SCCs as compared to normal epidermis with four previously published YAP gene signatures. These YAP signatures were obtained by transcriptional profiling human breast cell line MCF10A following YAP overexpression [39], a mouse model of hepatocellular carcinoma that presents YAP activation [40], human colorectal cancers expressing YAP [41], and oral squamous cell carcinoma cell line following YAP knockdown [42].

We compared the genes upregulated in FACS-isolated SmoM2-expressing cells in BCC in comparison with IFE, the compartment of the skin from which BCC originates in this model [28]. We found that BCC presented a strong enrichment for three out of the four YAP gene signatures (Fig 2). We found that FACS-isolated YFP^+ $Epcam^+$ cells from *Lgr5CREER/Kras^{G12D}/Tp53KO/Rosa-YFP*-induced well-differentiated SCCs originating from the IFE and YFP^+ Epcam- cells from *Lgr5CREER/Kras^{G12D}/Tp53KO/Rosa-YFP*-induced mesenchymal-like SCC arising from the HF [33] presented an enrichment for the four YAP gene signatures (Fig 2).

To confirm the significance of enrichment scores obtained from GSEA of the YAP genes signatures, we performed GSEA using Wnt and TGFβ pathways, two signaling pathways that regulate skin tumorigenesis [28,43–47]. Using GSEA, we compared BCC and SCC signatures with published Wnt and TGFβ signatures obtained from skin cancers [28,46]. These analyses confirmed the enrichment of Wnt signature in BCC and mesenchymal and well-differentiated SCC (Fig EV1A). The normalized enrichment score (NES) obtained in Wnt signature-SCC is comparable with those obtained in YAP-SCC. A higher NES was obtained in Wnt-BCC GSEA (Fig EV1A). Moreover, GSEA showed enrichment in BCC and mesenchymal SCC for TGFβ signature, with a NES comparable to those obtained for the YAP signatures. There was no enrichment of the TGFβ signature in *Lgr5CREER/Kras^{G12D}/Tp53KO/Rosa-YFP*-induced well-differentiated SCC (Fig EV1B). Altogether, these data indicate that YAP activation has an important impact on the gene expression profile of BCC and SCC tumor cells (Fig 2).

To determine whether BCC and SCC present common YAP downstream targets, we compared the genes upregulated in BCCs and SCCs with the four YAP published signatures. Interestingly, the importance of the overlap between the different YAP signatures differed with the different cancers (Fig 3A). A higher overlap was found between oral SCC and breast cancer YAP signatures (YAP Signature 1) [39,42]; and between hepatocellular carcinoma and colorectal cancer YAP signatures [40,41] (YAP Signature 2) (Fig 3B). For this reason, we compared the genes upregulated in BCC and SCC [28,33] with YAP signature 1 and YAP signature 2 separately (Fig 3C–H). Only 11 genes were upregulated in BCC and the YAP signature 1 (11/163: 7% of the YAP signature 1), including established direct targets of YAP and TAZ (*Ctgf* and *Cyr61*) [24], genes regulating cell proliferation (*Ccnd1*) and signaling pathways (*Wnt5a, Lifr, Tgfb2*), extracellular matrix (*Ctgf, Adamts1, Cyr61*) (Fig 3C). YAP signature 1 presented a higher overlap with genes upregulated in well-differentiated (73/163: 45%) and EMT-containing SCCs (38/163: 23%), including genes regulating cell cycle (*Aurkb, Cdkn3, Ccnb1, Cdc20, Prc1*) and DNA replication (*Blm, Mcm10, Gins1, Rfc4, Cdc6*) (Fig 3D). Only three genes of the YAP signature 1 (3/163: 2%) were commonly upregulated in BCC and mesenchymal and well-differentiated SCC, including *Cyr61*, a previously established YAP and TAZ direct target gene, *Wnt5a*, a non-canonical Wnt ligand and *Plod2*, an enzyme that mediates the formation of the stabilized collagen cross-links (Fig 3E).

A bigger overlap was found between genes upregulated in BCC and the genes of the YAP signature 2 (63/317: 20%), including *Cyr61* and genes involved in extracellular matrix regulation (*Fbln2, Fbln1, Col6a1, Ctgf*), extracellular exosome (*Crim1, S100a6, Cstb*), or Wnt signaling pathway (*Bgn, Sox4, Sox9, Timp3*; Fig 3F). This second YAP signature also significantly overlapped with genes upregulated in both well-differentiated (113/317: 36%) and EMT-containing SCCs (97/317: 30%), including genes regulating extracellular matrix remodeling (*Col6a3, Col6a1, Col3a1, Fbn1, Loxl1, Bgn, Timp1, Nid1*), genes involved in oxidative stress response (*Cyp1b1, Scara3, Gpx4, Gpx7, Gstm5*), immune response (*CD14, C1qa, C1qb, C1qc, Slpi*), and interferon response (*Ifitm3, Ifit2, Osmr*) (Fig 3G). A higher overlap of 20 genes (20/317: 6%) was found between the second YAP signature and the genes commonly upregulated in BCC and SCC, including *S100a8, Emp3, Fblim1, Rab31, Fstl1, Tmem98, Lcn2, Fxyd5, Socs3, Cstb, Slpi, Tes, Casp1,* and genes involved in extracellular matrix function (*Bgn, Fbln2, Slpi, Col6a1, and Cyr61*; Fig 3H). These results indicate that SCCs and BCCs present higher overlap with the colorectal and hepatocellular carcinoma YAP signatures (YAP signature 2) than with breast and oral SCC YAP signatures (YAP signature 1) and that well-differentiated SCCs present a much higher overlap than BCCs with the YAP signature from oral SCC, suggesting the existence of a common and tumor-specific sets of YAP target genes.

YAP and TAZ are essential for BCC initiation

To study the role of YAP and TAZ in BCC initiation, we deleted *YAP* and *TAZ* at the same time that we expressed the SmoM2 oncogene in the basal cells of the epidermis using the *K14CREER* (Fig 4A). *K14CREER/SmoM2-YFP/YAPfl/flTAZfl/fl* will be referred after TAM treatment as *SmoM2 YAP* and *TAZ DKO* thereafter. In this SmoM2-induced BCC mouse model, SmoM2 is fused to the yellow fluorescent protein (YFP); and therefore, the presence of SmoM2 oncogene-expressing cells can be monitored by the expression of YFP. We treated the mice with 20 mg tamoxifen to recombine SmoM2 and the other floxed alleles in the majority of epidermal basal cells. At the end of tamoxifen treatment in *K14CREER/SmoM2* mice (referred as *SmoM2* thereafter), SmoM2 is expressed in the majority of basal epidermal cells, hyperplasia could be observed after 2 weeks, which evolved toward dysplasia before progressing into BCC around 8 weeks of tamoxifen administration [30,48] (Fig 4B). *SmoM2 YAP* and *TAZ DKO* did not present any BCC 8 weeks following TAM administration (Fig 4B). Surprisingly, only rare SmoM2-expressing cells were observed in *SmoM2 YAP* and *TAZ DKO* epidermis at 2 and 8 weeks following tamoxifen administration (Fig 4C). To assess whether the rare SmoM2-expressing dysplastic lesions found in *SmoM2 YAP* and *TAZ DKO* epidermis resulted from the incomplete deletion of the YAP- and TAZ-floxed alleles, we assessed the expression of YAP

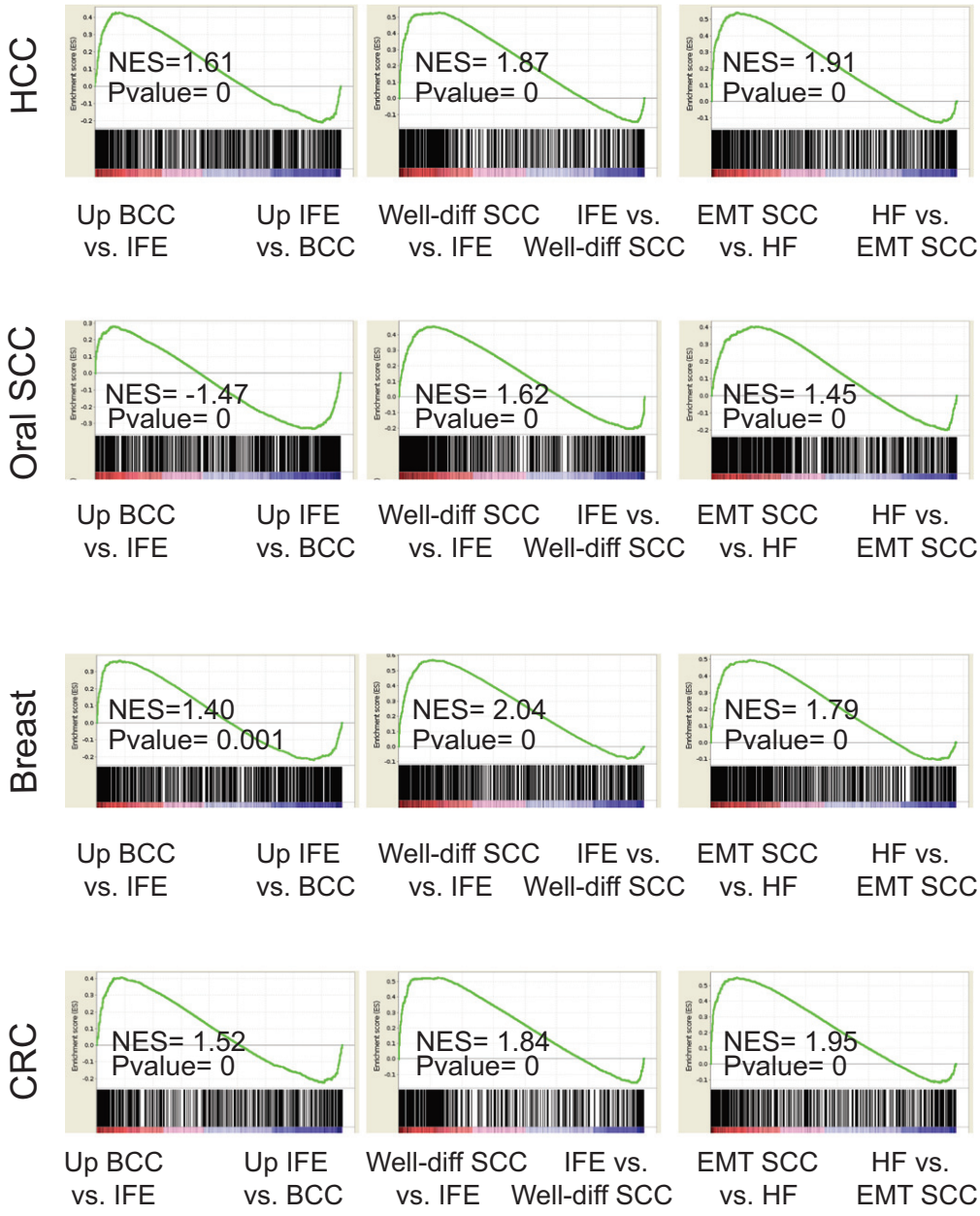

Figure 2. Mouse BCCs and SCCs express YAP gene signatures.

GSEA showing enrichment of BCC [28], well-differentiated and EMT-containing SCC [33] for YAP gene signatures obtained from mouse hepatocellular carcinoma [40] human breast cancer cell line [39], human oral squamous cell carcinoma [42], and human colorectal cancer [41]. Well-diff SCC: well-differentiated SCC; EMT SCC: EMT-containing SCC. Enrichment score and *P*-value were calculated using GSEA preranked module of GSEA software.

Source data are available online for this figure.

and TAZ by IHC in *SmoM2 YAP* and *TAZ DKO* epidermis 8 weeks following tamoxifen administration. YAP and TAZ expression was observed in the rare dysplastic lesions found in *SmoM2 YAP* and *TAZ DKO* epidermis, indicating that these lesions were formed by the rare SmoM2-expressing cells that escape complete *YAP* and *TAZ* deletion (Fig 4D). Altogether, these results indicate that YAP and TAZ are essential for SmoM2-induced BCC formation and the long-term maintenance of SmoM2-expressing cells. The presence of nuclear YAP in all mouse BCC and the absolute requirement of YAP and TAZ function for mouse BCC initiation suggest that YAP and TAZ activation does not require additional somatic mutations in this context. Similarly to BCC formation, activation of hedgehog signaling pathway in cerebellar granule neuron precursors (CGNPs) leads to medulloblastoma formation, a brain tumor occurring in children [49,50]. Interestingly, YAP1 expression is also upregulated in medulloblastoma of the SHH and WNT subtypes [51,52]. Culture CGNPs in the presence of SHH leads to

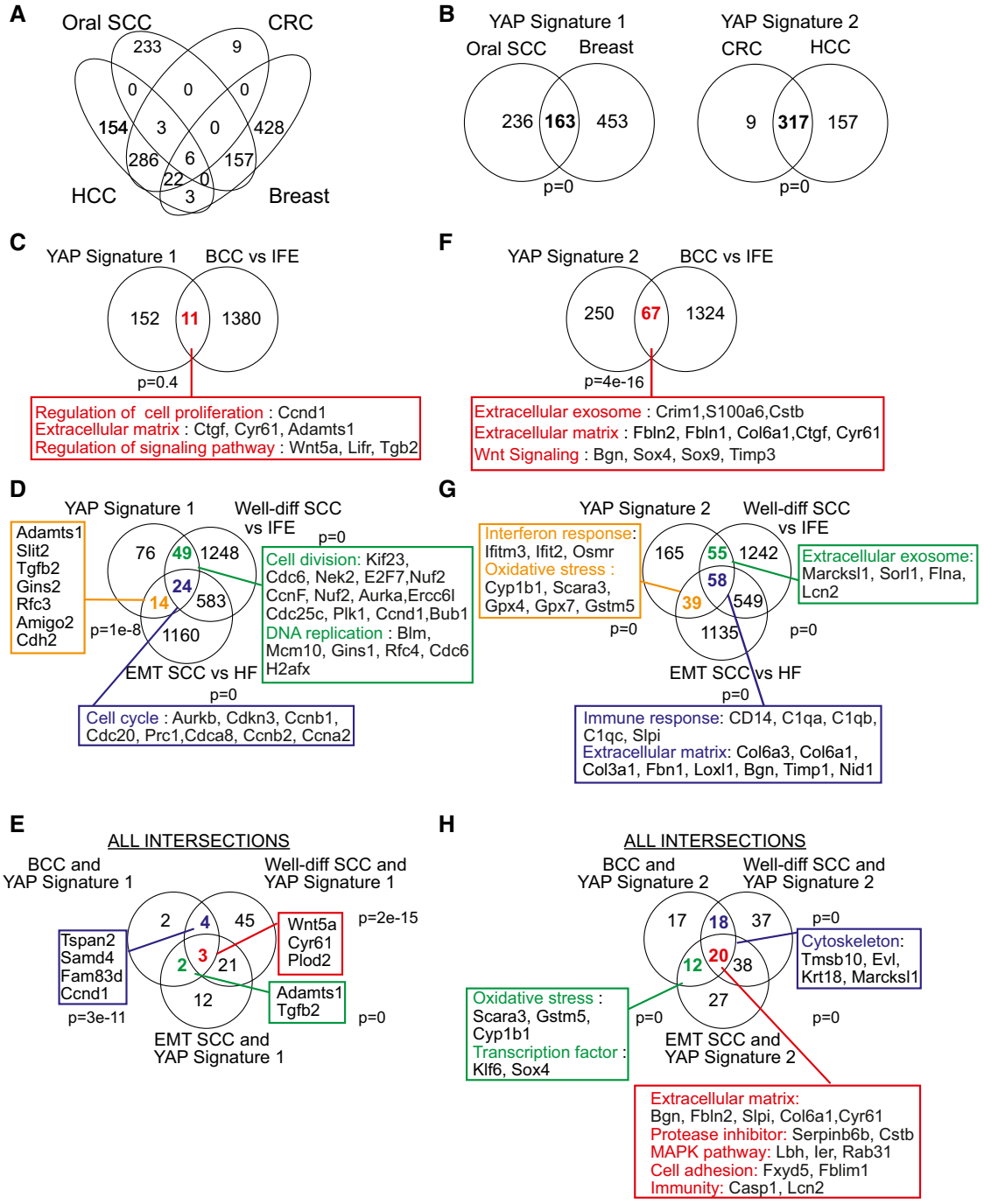

Figure 3. Expression of YAP signatures in mouse BCCs and SCCs.

A Venn diagram showing the overlap between four published YAP signatures [39–42].

B Venn diagram showing the overlap between the YAP signatures obtained in oral SCC and breast (YAP Signature 1) and CRC and HCC (YAP Signature 2).

C Venn diagram showing the overlap between YAP signature 1 and the genes upregulated by more than 1.5-fold in BCC compared to IFE [28].

D Venn diagram showing the overlap between YAP signature 1 and the genes upregulated by more than 1.5-fold in well-differentiated SCC versus IFE and in EMT-containing SCC versus HF [33].

E Venn diagram showing the genes commonly upregulated in YAP signature 1 and in BCCs, well-differentiated and EMT-containing SCCs.

F Venn diagram showing the overlap between YAP signature 2 and the genes upregulated by more than 1.5-fold in BCC compared to IFE [28].

G Venn diagram showing the overlap between YAP signature 2 and the genes upregulated by more than 1.5-fold in well-differentiated SCC versus IFE and in EMT-containing SCC versus HF [33].

H Venn diagram showing the genes commonly upregulated in YAP Signature 2 and in BCCs, well-differentiated and EMT-containing SCCs.

Data information: HCC: hepatocellular carcinoma; CRC: colorectal cancer; Well-diff SCC: well-differentiated SCC; EMT SCC: EMT-containing SCC. Hypergeometric test was used to assess the statistical significance.
Source data are available online for this figure.

YAP1 expression and nuclear localization leading to CGNP proliferation, suggesting that hedgehog signaling activation results in YAP activation [51]. One possible candidate that promotes YAP activation in BCC is Wnt signaling, as Wnt activation has been shown to promote YAP activation [10] and Wnt activation is rapidly activated following oncogenic hedgehog activation during the earliest step of BCC initiation [28,53]. In addition, BCC formation leads to cytoskeleton and extracellular matrix (ECM) remodeling [16] that could result in an increase in the stiffness of the ECM, which in turn can reinforce YAP1 activation [7,16].

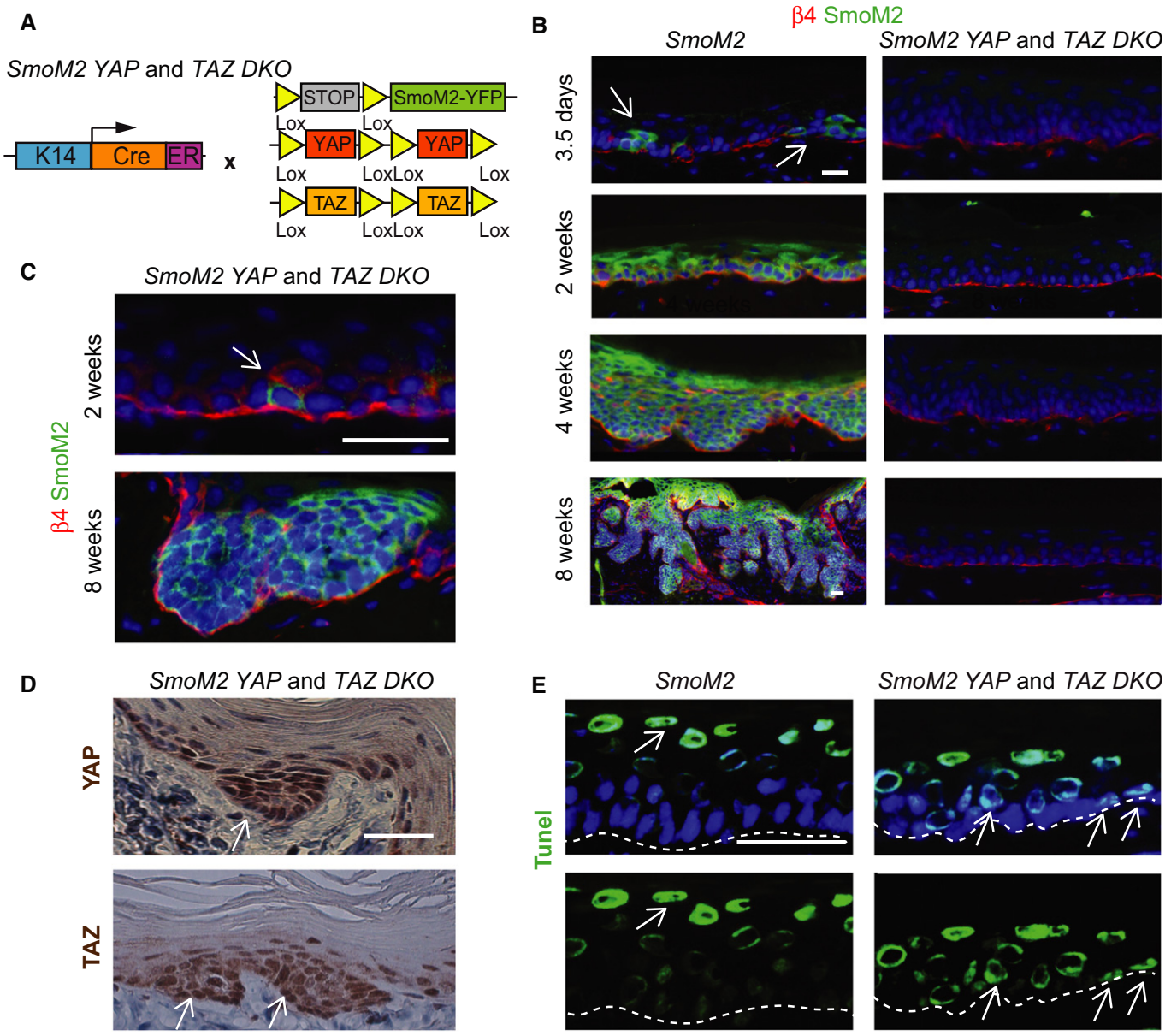

Figure 4. YAP and TAZ are required for BCC initiation.

A Scheme of the genetic strategy to delete *YAP* and *TAZ* and activate the oncogene SmoM2 in tumor-initiating cells.

B Immunostaining for SmoM2 and β4-integrin at different time points upon tamoxifen administration in *SmoM2 YAP* and *TAZ DKO* and *SmoM2* mice (n = 3 animals analyzed per genotype and time point). Arrows indicate SmoM2-expressing cells.

C Immunostaining for SmoM2 and β4-integrin in rare clones observed at 2 and 8 weeks after tamoxifen administration in *Smo2 YAP* and *TAZ DKO* mice. Arrows indicate SmoM2-expressing cells.

D Immunohistochemistry for YAP and TAZ in rare dysplasias observed in *SmoM2 YAP* and *TAZ DKO* mice 8 weeks after tamoxifen administration. Arrows indicate dysplasias presenting nuclear YAP and TAZ expression.

E TUNEL assay in *SmoM2 YAP* and *TAZ DKO* and *SmoM2* mice 3.5 days after tamoxifen administration. Arrows indicate TUNEL-positive cells and dashed line indicates the basal lamina.

Data information: Hoechst nuclear staining in blue. Scale bars: 20 μm.

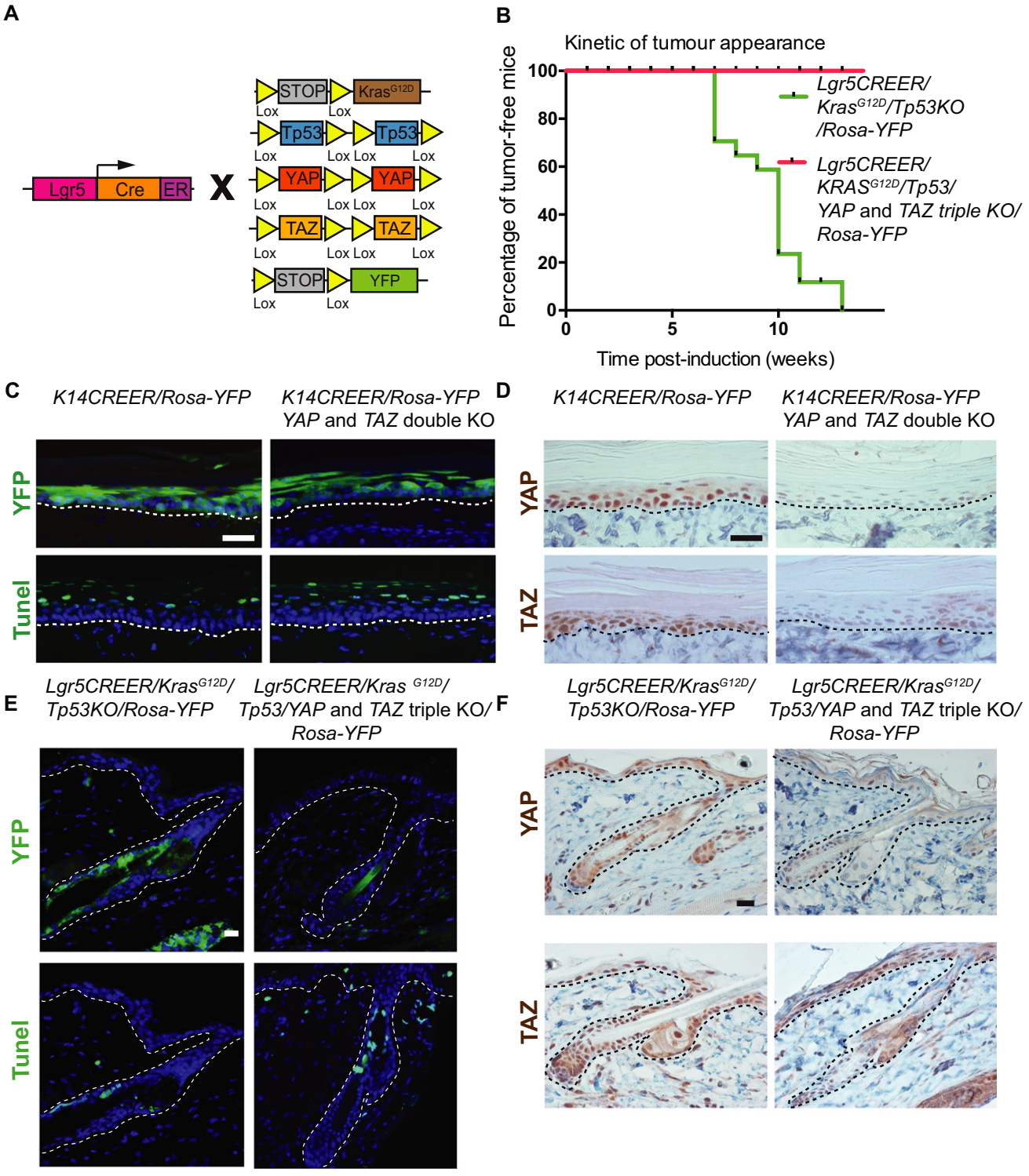

Figure 5. YAP and TAZ are required for the initiation of genetically induced SCC.

A Scheme of the genetic strategy to delete *YAP* and *TAZ* and activate the expression of oncogenic *Kras* and *Tp53* deletion in tumor-initiating cells.

B Kinetic of tumor appearance in *Lgr5CREER/Kras^{G12D}/Tp53 KO/Rosa-YFP* and *Lgr5CREER/Kras^{G12D}/Tp53/YAP/TAZ triple KO/Rosa-YFP* mice (n = 6 animals analyzed per genotype).

C, D Immunostaining for YFP and TUNEL assay (C) and immunohistochemistry for YAP and TAZ (D) in *K14CREER/YAP TAZ DKO/Rosa-YFP* mice and *K14CREER/Rosa-YFP* control mice.

E, F Immunostaining of YFP and TUNEL assay (E) and immunohistochemistry of YAP and TAZ (F) in *Lgr5CREER/Kras^{G12D}/Tp53KO/Rosa-YFP* mice and *Lgr5CREER/Kras^{G12D}/Tp53/YAP/TAZ triple KO/Rosa-YFP* mice 3.5 days after tamoxifen administration.

Data information: Scale bars: 20 μm. Dashed lines indicate the basal lamina.

To determine whether and how rapidly YAP and TAZ expression are required for the survival of SmoM2-expressing cells, we performed TUNEL assay to monitor cell death in the skin of *SmoM2* and *SmoM2 YAP* and *TAZ DKO* mice 3.5 days upon tamoxifen administration. In SmoM2-expressing cells, TUNEL-positive cells were only found in the suprabasal layers of the epidermis (Fig 4E). In contrast, in *SmoM2 YAP* and *TAZ DKO* mice, many basal cells characterized by their ring-shaped and the absence of nuclear staining, were TUNEL-positive, and these TUNEL-positive cells extended to the suprabasal layers (Fig 4E), suggesting that YAP and TAZ expression is required for the immediate survival of oncogene-expressing cells and the combination of SmoM2 expression with *YAP* and *TAZ* deletion is synthetic lethal.

YAP and TAZ are essential for SCC initiation

Whereas YAP and TAZ deletion inhibits the formation of benign papilloma following chemical-induced carcinogenesis [24] and the overexpression of phospho-mutant of YAP promotes skin tumor formation [8], it remains unclear whether YAP and TAZ are required for SCC initiation in genetically engineered SCC mouse model. To determine the importance of YAP and TAZ for SCC initiation, we induced the deletion of *YAP*, *TAZ* and *Tp53* together with $Kras^{G12D}$ expression in hair follicle cells using *Lgr5CREER* mice (Fig 5A). In the presence of YAP and TAZ expression, administration of 10 mg TAM to *Lgr5CREER/*$Kras^{G12D}$*/Tp53KO/Rosa-YFP* mice leads to the development of several tumors per mouse within 6–14 weeks after tamoxifen administration [33,34] (Fig 5B). However, no SCC was observed in the *Lgr5CREER/*$Kras^{G12D}$*/Tp53/YAP/TAZ triple KO/Rosa-YFP* mice during the next 15 weeks after tamoxifen administration (Fig 5B). These results reveal that YAP and TAZ are required for SCC initiation. *YAP* knockdown inhibits the growth of transplanted cervix and head and neck SCC cell lines [17], suggesting that targeting YAP could not only be beneficial for tumor initiation but also for the treatment of established tumors. YAP and TAZ are co-activators that form complexes with TEAD transcription factors and activate the expression of different target genes and downstream signaling pathways [6]. ATAC-seq and Chip-Seq have revealed that during Ras-induced tumorigenesis in eye-antennal imaginal disk tumor in flies, in mouse SCCs, and in melanoma, the active enhancers in these tumors contain frequently binding sites for AP1 and TEAD transcription factors, suggesting that YAP co-operate with JUN and FOS transcription factors to promote chromatin remodeling and gene expression in tumor cells [24,33,54,55]. Further studies will be required to determine which TEAD factors are mediating tumorigenesis in the different types of cancers and what are the other transcription factors that co-operate with YAP and TAZ to promote chromatin remodeling and tumorigenesis.

To determine whether and how rapidly YAP and TAZ expression are required for the survival of *Lgr5CREER/*$Kras^{G12D}$*/Tp53KO/Rosa-YFP*-expressing cells, we performed YFP and TUNEL immunostaining to monitor the fate of oncogene-expressing cells in the skin 3.5 days after tamoxifen administration. In the absence of oncogene expression, the deletion of *YAP* and *TAZ* was not essential for the survival of skin epidermal cells as demonstrated by the presence of YFP-positive cells, in which *YAP* and *TAZ* have been deleted without obvious signs of cell death (Fig 5C and D). Expression of oncogenic *Kras* and *Tp53* deletion in HF lineages did not lead to apoptotic or TUNEL-positive cells in YFP-positive cells (Fig 5E). In contrast, upon *YAP* and *TAZ* deletion in *Lgr5CREER/*$Kras^{G12D}$*/Tp53/YAP/TAZ triple KO/Rosa-YFP*, no YFP-positive cells could be observed together with a concomitant increase in TUNEL-positive cells, indicating that simultaneous activation of $Kras^{G12D}$ and deletion of *YAP* and *TAZ* leads to cell death (Fig 5E and F), suggesting that *YAP* and *TAZ* deletion is synthetically lethal in $Kras^{G12D}$*/Tp53 KO* cells, similarly as in SmoM2-expressing cells (Fig 4E).

Conclusions

Our study demonstrates that YAP and TAZ are essential for BCC and SCC initiation. Additional studies are required to elucidate whether targeting YAP and TAZ/TEAD alone or in combination in established tumor are sufficient to promote tumor regression and whether the synthetic lethality between oncogenic hedgehog or oncogenic Ras and *YAP* and *TAZ* deletion can be exploited to prevent the formation of new tumors in patients at high risk of forming BCCs and SCCs.

Materials and Methods

Mice

K14CREER transgenic mice [56] were kindly provided by E. Fuchs, Rockefeller University, USA. *Ptch1 fl/fl* mice [57], *Rosa26-SmoM2-YFP* [58], *Rosa26-YFP* [59], *Lgr5CREER* [60], $Kras^{LSL\text{-}G12D}$ [61], and TP53 fl/fl [62]mice have been received from the NCI mouse repository and the Jackson Laboratories. *YAP fl/fl* and *TAZ fl/fl* mice [63] were obtained from Georg Halder (KU Leuven) who received them from Randy Johnson at the MD Anderson Cancer Center, Houston. Mouse colonies were maintained in a certified animal facility in accordance with European guidelines. Experiments involving mice presented in this work were approved by Comité d'Ethique du Bien Être Animal (Université Libre de Bruxelles) under protocol number 434N, 483N, and 632N. Female and male animals have been used for all experiments, and equal animal gender ratios have been respected in the majority of the analysis, analysis of the different mutant mice was not blind, and sample size was calculated to reach statistical significance. The experiments were not randomized.

Human tissue samples

Twelve human normal skin samples as well as 10 actinic keratosis, 32 basal cell carcinoma (BCC) including superficial, nodular and infiltrative variants, 25 skin squamous cell carcinoma (SCC) including *in situ* and invasive variants, 11 lung SCC, 13 head and neck SCC, nine esophagus SCC and four cervix SCC were selected from archival formalin-fixed and paraffin-embedded (FFPE) human samples in the Erasme Hospital Biobank, Brussels, Belgium (BE_BERA1; Biobanque Hôpital Erasme-ULB (BERA); BE_NBWB1; Biothèque Wallonie Bruxelles (BWB); BBMRI-ERIC).

Mice induction with tamoxifen

For *Ptch1* deletion, *K14CREER/Ptch1fl/fl* mice (2.5 months old) received one intraperitoneal injection of 2.5 mg of tamoxifen during

three consecutive days. *SmoM2 YAP* and *TAZ* DKO and *SmoM2* mouse received one intraperitoneal injection of 2.5 mg tamoxifen during 10 consecutive days. *Lgr5CREER/Kras^{G12D}/Tp53fl/fl/Rosa-YFP* mice and *Lgr5CREER/Kras^{G12D}/Tp53fl/fl/YAPfl/fl TAZfl/fl* were injected intraperitoneally with 2.5 mg tamoxifen per day for 4 days beginning at P28. Tamoxifen was diluted in 90% sunflower oil and 10% ethanol.

Immunostaining in mouse skin sections

The tail and back skin of the mice were embedded in optimal cutting temperature compound (OCT, Sakura) and cut into 5–8 μm frozen sections using a CM3050S Leica cryostat (Leica Microsystems). Owing to the fusion of SmoM2 with YFP, SmoM2-expressing cells were detected using anti-GFP antibody. Frozen sections were dried and fixed with 4% paraformaldehyde/PBS (PFA) for 10 min at room temperature in the *SmoM2* mouse model. Skin from *Rosa-YFP* mice was pre-fixed for 2 h in 4% PAF before embedding in OCT and being sectioned. Then, sections were blocked using blocking buffer for 1 h (PBS, horse serum 5%, BSA 1%, Triton 0.1%). Skin sections were incubated with primary antibodies diluted in blocking buffer overnight at 4°C, washed with PBS for 3 × 5 min, and then incubated with Hoechst solution and secondary antibodies diluted in blocking buffer for 1 h at room temperature. Finally, sections were washed with PBS for 3 × 5 min at room temperature and mounted in DAKO mounting medium supplemented with 2.5% Dabco (Sigma). Primary antibodies used were the following: anti-B4-integrin (Rat, 1:200, BD, ref.553745) and anti-GFP (1:3,000, chicken, Abcam, ab13970). The following secondary antibodies were used: anti-chicken to AlexaFluor488 (Molecular Probes) and anti-rat to rhodamine Red-X (JacksonImmunoResearch). Detection of TUNEL-positive cells was performed using the *In Situ* Cell Death Detection kit (Roche) in samples that were fixed after sectioning. Images of the Immunostainings in sections were acquired using an Axio Imager M1 microscope, an AxioCamMR3 camera, and the Axiovision software (Carl Zeiss).

Immunohistochemistry murine samples

For YAP and TAZ immunohistochemistry in murine samples, paraffin sections were deparaffinized, rehydrated, followed by antigen unmasking performed for 20 min at 98°C in citrate buffer (pH 6) using the PT module. Endogenous peroxidase was blocked using 3% H_2O_2 (Merck) in methanol for 10 min at room temperature. Endogenous avidin and biotin were blocked using the Endogenous Blocking kit (Invitrogen) for 20 min at room temperature. Nonspecific antigen blocking was performed using blocking buffer. Rabbit anti-YAP (1/200, Santa Cruz Biotechnology) or Rabbit anti-TAZ (1/100, Sigma-Aldrich) were incubated overnight at 4°C. Anti-rabbit biotinylated with blocking buffer, Standard ABC kit, and ImmPACT DAB (Vector Laboratories) was used for the detection of horseradish peroxidase (HRP) activity. Slides were then dehydrated and mounted using SafeMount (Labonord).

Immunohistochemistry (IHC) human samples

Five-μm-thick sections of all samples were subjected to standard IHC on Ventana discovery XT (Ventana, Roche Diagnostics, Belgium) using the DABMap detection system according to manufacturer's recommendations. Briefly, the slides were incubated with the mouse monoclonal anti-YAP antibody for 12 h (1:75, clone G-6, Santa Cruz Biotechnology) or with the rabbit polyclonal anti-TAZ antibody for 1 h (1:200, Sigma-Aldrich, Missouri, USA). The slides were washed and incubated with the biotinylated anti-mouse secondary antibody (1:200, Vector Laboratories) followed by the addition of complex avidin-horseradish peroxidase. Immunostainings were detected by incubation with diaminobenzidine and hydrogen peroxide. Slides were counterstained with Gill's hematoxylin, dehydrated, and mounted. For each staining, an external positive control was included as well as a negative control, which entailed replacing the primary antibody with non-immune serum (Dako, Glostrup, Denmark).

GSEA

The GSEA program was downloaded from the BROAD Institute website (http://www.broadinstitute.org/gsea/). We used the GSEA *preranked* option with standard parameters of weighted enrichment score calculation to run the GSEA for four different signatures of YAP genes against a user-supplied fold-change-ranked list of genes (replicates from the same conditions are average, and then, we aggregate the different probes for the same gene by averaging them). NES is the normalized enrichment score.

Expanded View for this article is available online.

Acknowledgments
C.B. is an investigator of WELBIO. A.S-D. and M.D. are supported by a fellowship of the FNRS. S.R is funded by Fonds Yvonne Boël. Human IHC stainings were carried out at DiaPath, part of the CMMI. The CMMI is supported by the European Regional Development Fund. This work was supported by the FNRS, the WELBIO, the Fondation contre le Cancer, the ULB fondation, the Worldwide Cancer Research, the fondation Baillet Latour, and a consolidator grant of the European Research Council.

Author contributions
AS-D, MD, and CB designed the experiments, performed data analysis, and wrote the manuscript; SR and IS analyzed the human samples; MR helped in the homoeostasis experiments; ML and M-AP provided technical support, and AB performed the GSEA.

Conflict of interest
The authors declare that they have no conflict of interest.

References

1. Alam M, Ratner D (2001) Cutaneous squamous-cell carcinoma. *N Engl J Med* 344: 975 – 983
2. Epstein EH (2008) Basal cell carcinomas: attack of the hedgehog. *Nat Rev Cancer* 8: 743 – 754
3. Zanconato F, Cordenonsi M, Piccolo S (2016) YAP/TAZ at the roots of cancer. *Cancer Cell* 29: 783 – 803
4. Moroishi T, Hansen CG, Guan KL (2015) The emerging roles of YAP and TAZ in cancer. *Nat Rev Cancer* 15: 73 – 79
5. Halder G, Dupont S, Piccolo S (2012) Transduction of mechanical and cytoskeletal cues by YAP and TAZ. *Nat Rev Mol Cell Biol* 13: 591 – 600

6. Piccolo S, Dupont S, Cordenonsi M (2014) The biology of YAP/TAZ: hippo signaling and beyond. *Physiol Rev* 94: 1287 – 1312
7. Aragona M, Panciera T, Manfrin A, Giulitti S, Michielin F, Elvassore N, Dupont S, Piccolo S (2013) A mechanical checkpoint controls multicellular growth through YAP/TAZ regulation by actin-processing factors. *Cell* 154: 1047 – 1059
8. Schlegelmilch K, Mohseni M, Kirak O, Pruszak J, Rodriguez JR, Zhou D, Kreger BT, Vasioukhin V, Avruch J, Brummelkamp TR *et al* (2011) Yap1 acts downstream of alpha-catenin to control epidermal proliferation. *Cell* 144: 782 – 795
9. Camargo FD, Gokhale S, Johnnidis JB, Fu D, Bell GW, Jaenisch R, Brummelkamp TR (2007) YAP1 increases organ size and expands undifferentiated progenitor cells. *Curr Biol* 17: 2054 – 2060
10. Azzolin L, Panciera T, Soligo S, Enzo E, Bicciato S, Dupont S, Bresolin S, Frasson C, Basso G, Guzzardo V *et al* (2014) YAP/TAZ incorporation in the beta-catenin destruction complex orchestrates the Wnt response. *Cell* 158: 157 – 170
11. Cottini F, Hideshima T, Xu C, Sattler M, Dori M, Agnelli L, ten Hacken E, Bertilaccio MT, Antonini E, Neri A *et al* (2014) Rescue of Hippo coactivator YAP1 triggers DNA damage-induced apoptosis in hematological cancers. *Nat Med* 20: 599 – 606
12. Zhang H, Pasolli HA, Fuchs E (2011) Yes-associated protein (YAP) transcriptional coactivator functions in balancing growth and differentiation in skin. *Proc Natl Acad Sci USA* 108: 2270 – 2275
13. Elbediwy A, Vincent-Mistiaen ZI, Spencer-Dene B, Stone RK, Boeing S, Wculek SK, Cordero J, Tan EH, Ridgway R, Brunton VG *et al* (2016) Integrin signalling regulates YAP and TAZ to control skin homeostasis. *Development* 143: 1674 – 1687
14. Andl T, Zhou L, Yang K, Kadekaro AL, Zhang Y (2017) YAP and WWTR1: new targets for skin cancer treatment. *Cancer Lett* 396: 30 – 41
15. Quan T, Xu Y, Qin Z, Robichaud P, Betcher S, Calderone K, He T, Johnson TM, Voorhees JJ, Fisher GJ (2014) Elevated YAP and its downstream targets CCN1 and CCN2 in basal cell carcinoma: impact on keratinocyte proliferation and stromal cell activation. *Am J Pathol* 184: 937 – 943
16. Akladios B, Mendoza Reinoso V, Cain JE, Wang T, Lambie DL, Watkins DN, Beverdam A (2017) Positive regulatory interactions between YAP and Hedgehog signalling in skin homeostasis and BCC development in mouse skin *in vivo*. *PLoS One* 12: e0183178
17. He C, Mao D, Hua G, Lv X, Chen X, Angeletti PC, Dong J, Remmenga SW, Rodabaugh KJ, Zhou J *et al* (2015) The Hippo/YAP pathway interacts with EGFR signaling and HPV oncoproteins to regulate cervical cancer progression. *EMBO Mol Med* 7: 1426 – 1449
18. Silvis MR, Kreger BT, Lien WH, Klezovitch O, Rudakova GM, Camargo FD, Lantz DM, Seykora JT, Vasioukhin V (2011) Alpha-catenin is a tumor suppressor that controls cell accumulation by regulating the localization and activity of the transcriptional coactivator Yap1. *Sci Signal* 4: ra33
19. Liu T, Liu Y, Gao H, Meng F, Yang S, Lou G (2013) Clinical significance of yes-associated protein overexpression in cervical carcinoma: the differential effects based on histotypes. *Int J Gynecol Cancer* 23: 735 – 742
20. Xiao H, Wu L, Zheng H, Li N, Wan H, Liang G, Zhao Y, Liang J (2014) Expression of Yes-associated protein in cervical squamous epithelium lesions. *Int J Gynecol Cancer* 24: 1575 – 1582
21. Muramatsu T, Imoto I, Matsui T, Kozaki K, Haruki S, Sudol M, Shimada Y, Tsuda H, Kawano T, Inazawa J (2011) YAP is a candidate oncogene for esophageal squamous cell carcinoma. *Carcinogenesis* 32: 389 – 398
22. Song S, Honjo S, Jin J, Chang SS, Scott AW, Chen Q, Kalhor N, Correa AM, Hofstetter WL, Albarracin CT *et al* (2015) The Hippo coactivator YAP1 mediates EGFR overexpression and confers chemoresistance in esophageal cancer. *Clin Cancer Res* 21: 2580 – 2590
23. Li Z, Wang Y, Zhu Y, Yuan C, Wang D, Zhang W, Qi B, Qiu J, Song X, Ye J *et al* (2015) The Hippo transducer TAZ promotes epithelial to mesenchymal transition and cancer stem cell maintenance in oral cancer. *Mol Oncol* 9: 1091 – 1105
24. Zanconato F, Forcato M, Battilana G, Azzolin L, Quaranta E, Bodega B, Rosato A, Bicciato S, Cordenonsi M, Piccolo S (2015) Genome-wide association between YAP/TAZ/TEAD and AP-1 at enhancers drives oncogenic growth. *Nat Cell Biol* 17: 1218 – 1227
25. Jia J, Li C, Luo S, Liu-Smith F, Yang J, Wang X, Wang N, Lai B, Lei T, Wang Q *et al* (2016) Yes-associated protein contributes to the development of human cutaneous squamous cell carcinoma via activation of RAS. *J Invest Dermatol* 136: 1267 – 1277
26. Peterson SC, Eberl M, Vagnozzi AN, Belkadi A, Veniaminova NA, Verhaegen ME, Bichakjian CK, Ward NL, Dlugosz AA, Wong SY (2015) Basal cell carcinoma preferentially arises from stem cells within hair follicle and mechanosensory niches. *Cell Stem Cell* 16: 400 – 412
27. Wang GY, Wang J, Mancianti ML, Epstein EH Jr (2011) Basal cell carcinomas arise from hair follicle stem cells in Ptch1(+/–) mice. *Cancer Cell* 19: 114 – 124
28. Youssef KK, Lapouge G, Bouvree K, Rorive S, Brohee S, Appelstein O, Larsimont JC, Sukumaran V, Van de Sande B, Pucci D *et al* (2012) Adult interfollicular tumour-initiating cells are reprogrammed into an embryonic hair follicle progenitor-like fate during basal cell carcinoma initiation. *Nat Cell Biol* 14: 1282 – 1294
29. Kasper M, Jaks V, Are A, Bergstrom A, Schwager A, Svard J, Teglund S, Barker N, Toftgard R (2011) Wounding enhances epidermal tumorigenesis by recruiting hair follicle keratinocytes. *Proc Natl Acad Sci USA* 108: 4099 – 4104
30. Youssef KK, Van Keymeulen A, Lapouge G, Beck B, Michaux C, Achouri Y, Sotiropoulou PA, Blanpain C (2010) Identification of the cell lineage at the origin of basal cell carcinoma. *Nat Cell Biol* 12: 299 – 305
31. Wong SY, Reiter JF (2011) Wounding mobilizes hair follicle stem cells to form tumors. *Proc Natl Acad Sci USA* 108: 4093 – 4098
32. Bonilla X, Parmentier L, King B, Bezrukov F, Kaya G, Zoete V, Seplyarskiy VB, Sharpe HJ, McKee T, Letourneau A *et al* (2016) Genomic analysis identifies new drivers and progression pathways in skin basal cell carcinoma. *Nat Genet* 48: 398 – 406
33. Latil M, Nassar D, Beck B, Boumahdi S, Wang L, Brisebarre A, Dubois C, Nkusi E, Lenglez S, Checinska A *et al* (2017) Cell-type-specific chromatin states differentially prime squamous cell carcinoma tumor-initiating cells for epithelial to mesenchymal transition. *Cell Stem Cell* 20: 191 – 204.e5
34. Lapouge G, Beck B, Nassar D, Dubois C, Dekoninck S, Blanpain C (2012) Skin squamous cell carcinoma propagating cells increase with tumour progression and invasiveness. *EMBO J* 31: 4563 – 4575
35. Lapouge G, Youssef KK, Vokaer B, Achouri Y, Michaux C, Sotiropoulou PA, Blanpain C (2011) Identifying the cellular origin of squamous skin tumors. *Proc Natl Acad Sci USA* 108: 7431 – 7436
36. White AC, Tran K, Khuu J, Dang C, Cui Y, Binder SW, Lowry WE (2011) Defining the origins of Ras/p53-mediated squamous cell carcinoma. *Proc Natl Acad Sci USA* 108: 7425 – 7430
37. Shao DD, Xue W, Krall EB, Bhutkar A, Piccioni F, Wang X, Schinzel AC, Sood S, Rosenbluh J, Kim JW *et al* (2014) KRAS and YAP1 converge to regulate EMT and tumor survival. *Cell* 158: 171 – 184
38. Pastushenko I, Brisebarre A, Sifrim A, Fioramonti M, Revenco T, Boumahdi S, Van Keymeulen A, Brown D, Moers V, Lemaire S *et al*

(2018) Identification of the tumour transition states occurring during EMT. *Nature* 556: 463 – 468

39. Zhao B, Ye X, Yu J, Li L, Li W, Li S, Yu J, Lin JD, Wang CY, Chinnaiyan AM *et al* (2008) TEAD mediates YAP-dependent gene induction and growth control. *Genes Dev* 22: 1962 – 1971
40. Sohn BH, Shim JJ, Kim SB, Jang KY, Kim SM, Kim JH, Hwang JE, Jang HJ, Lee HS, Kim SC *et al* (2016) Inactivation of Hippo pathway is significantly associated with poor prognosis in hepatocellular carcinoma. *Clin Cancer Res* 22: 1256 – 1264
41. Lee KW, Lee SS, Kim SB, Sohn BH, Lee HS, Jang HJ, Park YY, Kopetz S, Kim SS, Oh SC *et al* (2015) Significant association of oncogene YAP1 with poor prognosis and cetuximab resistance in colorectal cancer patients. *Clin Cancer Res* 21: 357 – 364
42. Hiemer SE, Zhang L, Kartha VK, Packer TS, Almershed M, Noonan V, Kukuruzinska M, Bais MV, Monti S, Varelas X (2015) A YAP/TAZ-regulated molecular signature is associated with oral squamous cell carcinoma. *Mol Cancer Res* 13: 957 – 968
43. Yang SH, Andl T, Grachtchouk V, Wang A, Liu J, Syu LJ, Ferris J, Wang TS, Glick AB, Millar SE *et al* (2008) Pathological responses to oncogenic Hedgehog signaling in skin are dependent on canonical Wnt/beta3-catenin signaling. *Nat Genet* 40: 1130 – 1135
44. Malanchi I, Peinado H, Kassen D, Hussenet T, Metzger D, Chambon P, Huber M, Hohl D, Cano A, Birchmeier W *et al* (2008) Cutaneous cancer stem cell maintenance is dependent on beta-catenin signalling. *Nature* 452: 650 – 653
45. Schober M, Fuchs E (2011) Tumor-initiating stem cells of squamous cell carcinomas and their control by TGF-beta and integrin/focal adhesion kinase (FAK) signaling. *Proc Natl Acad Sci USA* 108: 10544 – 10549
46. Oshimori N, Oristian D, Fuchs E (2015) TGF-beta promotes heterogeneity and drug resistance in squamous cell carcinoma. *Cell* 160: 963 – 976
47. Larsimont JC, Youssef KK, Sanchez-Danes A, Sukumaran V, Defrance M, Delatte B, Liagre M, Baatsen P, Marine JC, Lippens S *et al* (2015) Sox9 controls self-renewal of oncogene targeted cells and links tumor initiation and invasion. *Cell Stem Cell* 17: 60 – 73
48. Sanchez-Danes A, Hannezo E, Larsimont JC, Liagre M, Youssef KK, Simons BD, Blanpain C (2016) Defining the clonal dynamics leading to mouse skin tumour initiation. *Nature* 536: 298 – 303
49. Yang ZJ, Ellis T, Markant SL, Read TA, Kessler JD, Bourboulas M, Schuller U, Machold R, Fishell G, Rowitch DH *et al* (2008) Medulloblastoma can be initiated by deletion of Patched in lineage-restricted progenitors or stem cells. *Cancer Cell* 14: 135 – 145
50. Schuller U, Heine VM, Mao J, Kho AT, Dillon AK, Han YG, Huillard E, Sun T, Ligon AH, Qian Y *et al* (2008) Acquisition of granule neuron precursor identity is a critical determinant of progenitor cell competence to form Shh-induced medulloblastoma. *Cancer Cell* 14: 123 – 134
51. Fernandez LA, Northcott PA, Dalton J, Fraga C, Ellison D, Angers S, Taylor MD, Kenney AM (2009) YAP1 is amplified and up-regulated in hedgehog-associated medulloblastomas and mediates Sonic hedgehog-driven neural precursor proliferation. *Genes Dev* 23: 2729 – 2741
52. Ellison DW, Dalton J, Kocak M, Nicholson SL, Fraga C, Neale G, Kenney AM, Brat DJ, Perry A, Yong WH *et al* (2011) Medulloblastoma: clinicopathological correlates of SHH, WNT, and non-SHH/WNT molecular subgroups. *Acta Neuropathol* 121: 381 – 396
53. Grachtchouk M, Mo R, Yu S, Zhang X, Sasaki H, Hui CC, Dlugosz AA (2000) Basal cell carcinomas in mice overexpressing Gli2 in skin. *Nat Genet* 24: 216 – 217
54. Atkins M, Potier D, Romanelli L, Jacobs J, Mach J, Hamaratoglu F, Aerts S, Halder G (2016) An ectopic network of transcription factors regulated by hippo signaling drives growth and invasion of a malignant tumor model. *Curr Biol* 26: 2101 – 2113
55. Verfaillie A, Imrichova H, Atak ZK, Dewaele M, Rambow F, Hulselmans G, Christiaens V, Svetlichnyy D, Luciani F, Van den Mooter L *et al* (2015) Decoding the regulatory landscape of melanoma reveals TEADS as regulators of the invasive cell state. *Nat Commun* 6: 6683
56. Vasioukhin V, Degenstein L, Wise B, Fuchs E (1999) The magical touch: genome targeting in epidermal stem cells induced by tamoxifen application to mouse skin. *Proc Natl Acad Sci USA* 96: 8551 – 8556
57. Uhmann A, Dittmann K, Nitzki F, Dressel R, Koleva M, Frommhold A, Zibat A, Binder C, Adham I, Nitsche M *et al* (2007) The hedgehog receptor patched controls lymphoid lineage commitment. *Blood* 110: 1814 – 1823
58. Mao J, Ligon KL, Rakhlin EY, Thayer SP, Bronson RT, Rowitch D, McMahon AP (2006) A novel somatic mouse model to survey tumorigenic potential applied to the Hedgehog pathway. *Cancer Res* 66: 10171 – 10178
59. Srinivas S, Watanabe T, Lin CS, William CM, Tanabe Y, Jessell TM, Costantini F (2001) Cre reporter strains produced by targeted insertion of EYFP and ECFP into the ROSA26 locus. *BMC Dev Biol* 1: 4
60. Barker N, van Es JH, Kuipers J, Kujala P, van den Born M, Cozijnsen M, Haegebarth A, Korving J, Begthel H, Peters PJ *et al* (2007) Identification of stem cells in small intestine and colon by marker gene Lgr5. *Nature* 449: 1003 – 1007
61. Tuveson DA, Shaw AT, Willis NA, Silver DP, Jackson EL, Chang S, Mercer KL, Grochow R, Hock H, Crowley D *et al* (2004) Endogenous oncogenic K-ras(G12D) stimulates proliferation and widespread neoplastic and developmental defects. *Cancer Cell* 5: 375 – 387
62. Jonkers J, Meuwissen R, van der Gulden H, Peterse H, van der Valk M, Berns A (2001) Synergistic tumor suppressor activity of BRCA2 and p53 in a conditional mouse model for breast cancer. *Nat Genet* 29: 418 – 425
63. Xin M, Kim Y, Sutherland LB, Murakami M, Qi X, McAnally J, Porrello ER, Mahmoud AI, Tan W, Shelton JM *et al* (2013) Hippo pathway effector Yap promotes cardiac regeneration. *Proc Natl Acad Sci USA* 110: 13839 – 13844

